BIOLOGY OF REPRODUCTION (2016) **94**(2):44, 1–12
Published online before print 6 January 2016.
DOI 10.1095/biolreprod.115.133058

Growth Arrest Specific-1 (GAS1) Is a C/EBP Target Gene That Functions in Ovulation and Corpus Luteum Formation in Mice[1]

Yi A. Ren,[3] Zhilin Liu,[3] Lisa K. Mullany,[3] Chen-Ming Fan,[4] and JoAnne S. Richards[2,3]

[3]*Department of Molecular and Cellular Biology, Baylor College of Medicine, Houston, Texas*
[4]*Department of Embryology, Carnegie Institution of Washington, Baltimore, Maryland*

ABSTRACT

Ovulation and luteinization are initiated in preovulatory follicles by the luteinizing hormone (LH) surge; however, the signaling events that mediate LH actions in these follicles remain incompletely defined. Two key transcription factors that are targets of LH surge are C/EBPalpha and C/EBPbeta, and their depletion in granulosa cells results in complete infertility. Microarray analyses of these mutant mice revealed altered expression of a number of genes, including growth arrest specific-1 (*Gas1*). To investigate functions of *Gas1* in ovulation- and luteinization-related processes, we crossed *Cyp19a1-Cre* and *Gas1*$^{flox/flox}$ mice to conditionally delete *Gas1* in granulosa and cumulus cells. While expression of *Gas1* is dramatically increased in granulosa and cumulus cells around 12–16 h post-human chorionic gonadotropin (hCG) stimulation in wild-type mice, this increase is abolished in *Cebpa/b* double mutant and in *Gas1* mutant mice. GAS1 is also dynamically expressed in stromal cells of the ovary independent of C/EBPalpha/beta. Female *Gas1* mutant mice are fertile, exhibit enhanced rates of ovulation, increased fertility, and higher levels of *Areg* and *Lhcgr* mRNA in granulosa cells. The morphological appearance and vascularization of corpora lutea appeared normal in these mutant females. Interestingly, levels of mRNA for a number of genes (*Cyp11a1, Star, Wnt4, Prlr, Cd52,* and *Sema3a*) associated with luteinization are decreased in corpora lutea of *Gas1* mutant mice as compared with controls at 24 h post-hCG; these differences were no longer detectable by 48 h post-hCG. The C/EBP target *Gas1* is induced in granulosa cells and is associated with ovulation and luteinization.

C/EBP alpha, C/EBP beta, corpus luteum, Gas1, *ovulation*

INTRODUCTION

The processes of ovulation and luteinization are initiated by the release of the luteinizing hormone (LH) surge from the pituitary. LH binds to its cognate G-protein coupled receptors present in theca cells and granulosa cells of large antral, preovulatory follicles [1] and stimulates a cascade of intrafollicular and intracellular events that lead to ovulation and corpus luteum (CL) formation [2]. Of particular relevance is the induction by LH of the epidermal growth factor (EGF)-like factors amphiregulin, epiregulin, and betacellulin [3] that activate the EGF-receptors and downstream regulatory kinases, MAPK3/1 (also known as ERK1/2) [4–8]. Targets of MAPK3/1 include the transcription factors CCAAT enhancer binding proteins alpha and beta (C/EBPα and C/EBPβ) [3]. Targeted disruption of the *Cebpa* and *Cebpb* genes selectively in granulosa cells of antral follicles in mice has documented that they are essential for both ovulation and luteinization [9, 10].

C/EBPα/ or C/EBPβ are activated selectively during inflammatory responses in the liver [11], during adipocyte differentiation [12, 13], in macrophages [12], during the uterine decidual response [14, 15], and by LH during ovulation [10, 16]. Microarray analyses of RNA prepared from granulosa cells of wild-type and *Cebpa/b*$^{fl/fl}$*;Cyp19a1-Cre* mutant mice have identified known and novel genes that are either up- or down-regulated by the deletion of these transcription factors [10], such as down-regulated expression of the prolactin receptor (*Prlr*) [10], the multidrug transporter *Abcb1b1* and plexin D1 (*Plxnd1*) [10], and up-regulated expression of inhibin (*Inha*) [17] and aromatase (*Cyp19a1*) [9]. Putative C/EBP binding sites have been identified in the promoters of these genes, indicating that they are likely to be direct targets of these transcription factors [18, 19]. One novel gene that we identified in the *Cebpa/b*$^{fl/fl}$*;Cyp19a1-Cre* mutant ovary microarray is growth arrest specific-1 (*Gas1*) [10]. The *Gas1* gene also has potential C/EBP binding sites [18, 19] and is markedly reduced in granulosa cells of the *Cebpa/b*$^{fl/fl}$*;Cyp19a1-Cre* mutant mice [10].

GAS1 is a glycosyl phosphatidylinositol-linked membrane protein that is an important coordinator of cell proliferation and survival through multiple mechanisms, such as inhibiting DNA synthesis [20] and increasing apoptosis [21]. Overexpression of GAS1 documents that it has potent tumor suppressor functions and suppresses melanoma metastasis [22–24]. The physiological importance of GAS1 is much more complex as revealed by the phenotype of *Gas1* knockout mice [25–28]. During development, GAS1 appears to act, in part, as a coregulator of the morphogenic factors in the hedgehog (HH) signaling cascades [29]. In the developing somite, GAS1 is induced by WNT to attenuate cell response to SHH [30]. GAS1 has also been linked to the glial cell-derived neurotrophic factor (GDNF) and its receptor RET signaling cascade [31, 32]. In endothelial cells, GAS1 is induced by VE-cadherin and VEGF

[1]This work has been supported by NIH-CA-181808 (J.S.R.), NIH-HD-16229 (J.S.R.), U54-HD07945 (Project 2, J.S.R.), SCCPIR (to J.S.R.), Specialized Cooperative Centers Program in Reproduction and Infertility Research (Bert W. O'Malley, B.W.O.), NIH-T32-HD-001765-36 (B.W.O.), and NIH-RO1-DK084963 (C.M.F.). This project was also supported by the Integrated Microscopy Core at Baylor College of Medicine with funding from the NIH (HD007495, DK56338, and CA125123), the Dan L. Duncan Cancer Center, and the John S. Dunn Gulf Coast Consortium for Chemical Genomics as well as the Pathology and Histology Core at Baylor College of Medicine with funding from the NIH (NCI P30-CA125123). Presented as a poster in part at the 46th Annual Meeting of the Society for the Study of Reproduction, 22–26 July 2013, Montréal, Québec, Canada.
[2]Correspondence: JoAnne S. Richards, Department of Molecular and Cellular Biology, Baylor College of Medicine, Mail Stop 130, One Baylor Plaza, Houston, TX 77030. E-mail: joanner@bcm.edu

Received: 1 July 2015.
First decision: 4 August 2015.
Accepted: 30 December 2015.

eISSN: 1529-7268 http://www.biolreprod.org
ISSN: 0006-3363

through the PI3K pathway to inhibit endothelial cell apoptosis and may thus facilitate resting endothelium integrity [32]. Considering the wide range of functions of GAS1, it is not surprising that the majority of *Gas1* null mice die embryonically with multiple defects in retinal, cerebral, neural tube, limb, and cardiac development [25–28, 33].

Based on our evidence that *Gas1* expression was highly increased in granulosa cells of ovulating follicles [10] and that the promoter of the *Gas1* gene has putative C/EBPβ binding sites [34, 35], we hypothesized that *Gas1* is a C/EBPβ target gene in granulosa cells and might be critical for mediating specific events associated with ovulation and/or luteinization. GAS1 is also expressed in rat CL where it possibly impacts apoptosis during the demise of CL mediated by luteolytic events [36]. To address the potential roles of GAS1 in the mouse ovary, we have analyzed the temporal and spatial expression of *Gas1* mRNA and protein in ovarian cells in response to LH/hCG in wild-type and *Cebpa/b*$^{fl/fl}$*;Cyp19a1-Cre* mutant mice and determined the intraovarian localization of GAS1 protein before and following the exposure to an LH/hCG stimulus. Because the *Gas1* null mice die shortly after birth [25], *Gas1*$^{fl/fl}$ mice have been generated [37], allowing us to create granulosa cell- and cumulus cell-specific *Gas1* knockout mice with *Cyp19a1-Cre* mouse strain [38] and to analyze the impact of *Gas1* deletion on the processes of ovulation and luteinization.

MATERIALS AND METHODS

Animal Studies and Generation of Genetically Engineered Mouse Models

Gas1$^{fl/fl}$ mice have been generated to allow cell-specific disruption of the *Gas1* gene [37]. *Cebpa/b*$^{fl/fl}$*;Cyp19a1-Cre* mutant mice were generated as previously described [10]. For superovulation studies, mice were injected intraperitoneally with 5 IU equine chorionic gonadotropin (eCG) followed 48 h later with 5 IU hCG. Granulosa cells, cumulus cells, or whole ovaries were collected from these mice for subsequent analyses. All the animals were 1) housed under a 14L:10D schedule in the Center for Comparative Medicine at Baylor College of Medicine and provided food and water ad libitum and 2) maintained according to the National Institutes of Health (NIH) Guide for the Care and Use of Laboratory Animals and approved by the Animal Care and Use Committee at Baylor college of Medicine.

Histology, Immunofluorescence, and Immunohistochemistry

Ovarian tissues were fixed in 4% paraformaldehyde and either embedded in paraffin for routine histological (hematoxylin and eosin [H&E]) and immunofluorescent (IF) analyses or frozen in optimal cutting temperature compound (Ted Pella, Inc.) for other specific IF analyses. Primary antibodies specific for GAS1 (AF2644; R&D system), PTX3 (P0496; Sigma Aldrich), SFRP4 (HPA009712; Sigma Aldrich), PECAM-1 (553373; BD Pharmingen), and collagen IV (ab6586; Abcam) were used in the IF studies. Cell nuclei were counterstained with 5μg/ml Hoechst 33342 dye (Sigma Aldrich). Digital images of H&E and IF staining were captured using a Zeiss AxioPlan2 microscope in the Integrated Microscopy Core, and images of IF staining were captured with Zeiss LSM780 confocal microscope in the Optical Imaging and Vital Microscopy Core at Baylor College of Medicine.

RNA Extraction, Real-Time RT-PCR, and Microarray Analyses

Total RNA was extracted from granulosa cells, cumulus-oocyte-complexes (COCs), ovarian stromal tissue (residual tissues after removing granulosa cells via needle puncture of the ovary), isolated CL, or whole ovaries at different time intervals before and after ovulation. Total RNA extraction, reverse transcription, and real-time PCR were performed using procedure previously described [39]. Primers used for real-time RT-PCR are listed in Supplemental Table S1 (available online at www.biolreprod.org).

Western Blot Analyses

Granulosa, COCs, ovarian stromal tissue, or whole ovaries were lysed in RIPA buffer (Boston BioProducts). Proteins were separated using a 10% Bis-Tris gel and transferred to an immobilon-P membrane (Millipore). Primary antibodies used included GAS1 (1:1000 dilution, AF2644; R&D system) and AKT (1:2000 dilution, 9272; Cell Signaling Technology). Signals were detected using the Peirce ECL 2 Western Blotting Substrate (Thermo Scientific).

Measurement of Serum Progesterone

Blood was collected via heart puncture at 24 h post-hCG stimulation from mice anesthetized with isoflurane and spun down in a BD Microtainer serum collection tube (BD Pharmingen). All the sera were then shipped on dry ice to the University of Virginia Core Laboratory for hormone measuring.

DNA Extraction and PCR Verification of Gas1 Deletion in Gas1$^{fl/fl}$;Cyp19a1-Cre Mice

DNA was extracted from granulosa cells and COCs collected from wild-type, heterozygous, and homozygous mutant mice at 24 h post-hCG using QIAprep Spin Miniprep Kit (Qiagen). The DNA product from each mouse was then amplified using primers flanking the LoxP sites in the *Gas1*$^{fl/fl}$ allele (forward primer: 5′-gcggaactcggacaaact-3′; reverse primer: 5′-cctcaa catcccttctccaa-3′). After PCR amplification, the resultant DNA samples were purified with QIAquick Gel Extraction Kit (Qiagen) and submitted for sequencing or were resolved in a 2.5% agarose gel to verify the deletion of *Gas1* in the heterozygous and homozygous mice, respectively (wild type: 1458 bp; *Gas1* null: 375 bp). Results from sequencing also confirmed successful deletion of *Gas1* (data not shown).

Granulosa Cell Culture and In Vitro Deletion of Gas1 Using Cre-Expressing Adenovirus

Granulosa cells were collected from eCG-primed (24 h) 22–23 day-old mice and cultured in Dulbecco-modified Eagle medium nutrient mixture F-12 (DMEM/F12) (Life Technologies) supplemented with penicillin, streptomycin, and 5% fetal bovine serum (Life Technologies). After overnight culture, cells were cultured in DMEM/F12 supplemented with 10% fetal bovine serum for 1 h, then transfected with an adenoviral vector expressing CRE recombinase at 7.0×10^{11} plaque-forming units/ml (Ad5-CMV-Cre-eGFP, Vector Development Laboratory, Baylor College of Medicine). After 4 h of transfection, the transfection efficiency was examined under a fluorescent microscope according to eGFP expression (>90% transfection efficiency). Cells were then gently washed with DMEM/F12 and cultured for 1 h in DMEM/F12 supplemented with 5% fetal bovine serum before treatment with forskolin/phorbol 12-myristate 13-acetate (PMA) (Fo/PMA). Cells were harvested for RNA at 0 and 24 h of Fo/PMA treatment.

Statistics

Data are represented as mean ± SEM. Comparisons between two experimental groups were analyzed using unpaired Student *t*-test. Comparison between multiple experimental groups were analyzed using one way ANOVA and Tukey honest significant difference test. A two-tailed $P < 0.05$ was considered statistically significant.

RESULTS

LH/hCG Induce Expression of Gas1 mRNA and Protein in Granulosa Cells and Cumulus Cells

To determine the temporal pattern of *Gas1* mRNA expression in the murine ovary, granulosa cells (or whole ovaries at 24 h post-hCG) were isolated from ovaries of hormonally primed immature mice prior to and after 5 IU eCG to stimulate preovulatory follicle growth and at selected times after 5 IU hCG to initiate ovulation and luteinization [10]. COCs were also isolated from ovaries and the oviduct of the hormonally primed mice. Following hCG stimulation, *Gas1* mRNA was low from 2–8 h but increased markedly between 8–16 h post-hCG (Fig. 1A). *Gas1* mRNA exhibited a similar

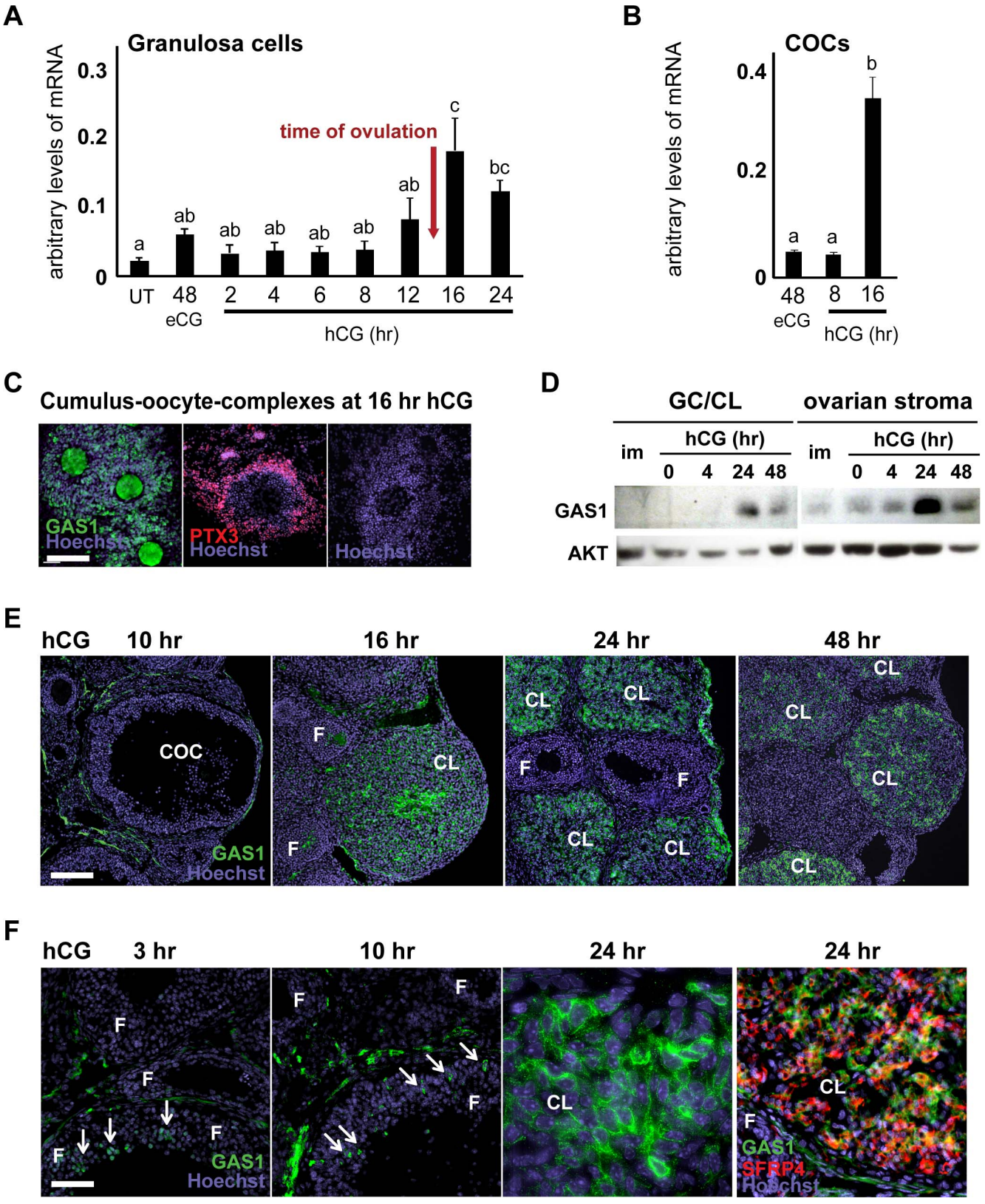

FIG. 1. Expression of *Gas1* was induced in granulosa cells and COCs around the time of ovulation. Levels of mRNA for *Gas1* increased in granulosa cells (**A**) and COCs (**B**) at ovulation as measured by real-time quantitative PCR. For both **A** and **B**, data shows mean ± SEM; n = 3. Bars without common superscripts are statistically different ($P < 0.05$). **C**) Immunofluorescent localization of GAS1 (green) and PTX3 (red) in ovulated COC collected from the oviduct at 16 h post-hCG. Bar = 100 μm. **D**) Western blot analyses of GAS1 and AKT in granulosa cells, luteal cells and ovarian stromal cells before and after ovulation. GC, granulosa cells; CL, corpus luteum. **E**) Immunofluorescent staining of GAS1 in the ovary before and after ovulation. Bar = 100 μm. **F**) Immunofluorescent staining showing GAS1 expression in sporadic granulosa cells (arrows) before ovulation (3 and 10 h post-hCG) and cytoplasmic membrane localization of GAS1 in luteinizing granulosa cells (24 h post-hCG). CL, corpus luteum. Bar = 50 and 10 μm. Expression of GAS1 (green) mostly colocalized with expression of SFRP4 (red) in luteinizing granulosa cells at 24 h post-hCG. CL, corpus luteum; F, follicle.

pattern in COCs with marked increases occurring between 8–16 h post-hCG.

GAS1 expression and localization in granulosa cells and COCs were examined further by IF staining. At 16 h post-hCG (Fig. 1C), COCs stained positively for GAS1 as well as pentraxin 3 (PTX3), a gene induced in COCs after the LH surge as shown previously [40, 41]. Oocytes also stained positive for GAS1 at this time but not in immature follicles. Western blot analyses demonstrated that while expression of GAS1 in stromal cells of the ovary was evident at all time points examined, GAS1 was detected with this method in luteal cells at 24 h post-hCG but not in granulosa cells at earlier time points (Fig. 1D). However, sporadic granulosa cells expressing GAS1 were detected using IF at 3 and 10 h post-hCG in preovulatory follicles (Fig. 1F). Because only a small number of granulosa cells expressed GAS1 before ovulation, it was not surprising that Western blot analysis did not detect GAS1 protein at these time points (Fig. 1D). In CL, GAS1 distinctly localized to the cytoplasmic membrane of luteal cells that also stain positive for a known luteal cell marker, SFRP4 (Fig. 1F, 24 h post-hCG) [42].

Induction of Gas1 *in Granulosa Cells and COCs by hCG Is Dependent on C/EBPα/β*

Our previous studies showed that selective depletion of *Cebpa* and *Cebpb* in granulosa cells of the *Cebpa/b*$^{fl/fl}$*;Cyp19a1-Cre* mice prevented ovulation and thus impaired fertility [10]. Microarray analyses further indicated that *Gas1* mRNA was reduced markedly in ovaries of the *Cebpa/b*$^{fl/fl}$*;Cyp19a1-Cre* mice [10]. Because ovulation and luteinization fail to occur in the *Cebpa/b*$^{fl/fl}$*;Cyp19a1-Cre* mutant mice, we were able to isolate granulosa cells from these mice and CL from wild-type controls to compare their mRNA and protein expression of selected genes. To verify and extend the above observations, CL (control mice, 24 h post-hCG), granulosa cells (mutant mice, 24 h post-hCG), and COCs (16 h post-hCG) were isolated from hormonally primed immature control and *Cebpa/b*$^{fl/fl}$*;Cyp19a1-Cre* mutant mice (Fig. 2A). *Gas1* mRNA was reduced markedly in granulosa cells and COCs of the *Cebpa/b*$^{fl/fl}$*;Cyp19a1-Cre* mutant mice compared to wild-type controls. Immunofluorescent analyses confirmed that GAS1 protein was not detectable in the granulosa cells of follicles that failed to ovulate in the *Cebpa/b*$^{fl/fl}$*;Cyp19a1-Cre* mutant mice (Fig. 2B) [10]. GAS1 was present and not reduced in cells within the stromal ovarian tissue between preovulatory follicles but was not detected in PECAM-1-positive endothelial cells in the ovarian stroma (Fig. 2C). These observations show that GAS1 is expressed in ovarian stromal cells surrounding follicles and luteinizing granulosa cells, and only the latter is dependent on C/EBPα/β.

We further investigated the ovarian stromal expression of GAS1 in ovaries from wild-type mice during different stages of follicular development using IF staining. In immature mice (Fig. 2D), no GAS1 was detected in granulosa cells, whereas intense staining was detected in stromal cells surrounding growing follicles. Some cells expressing GAS1 were adjacent to, but had minimal overlapping expression with, PECAM-1-positive endothelial cells. A similar pattern of GAS1 expression was also observed at 4 h post-hCG (Fig. 2E). Around the time of ovulation (12 h post-hCG) (Fig. 2F), sporadic GAS1-expressing cells were readily detected in the newly forming CL (FCL) sharing some overlap with collagen IV, a marker of vascular tissue. Strong expression of GAS1 also remained present in the stromal cells. However, at 24 and 48 h post-hCG, GAS1 expression in ovarian stromal cells appeared less prominent (but still detectable via IF staining) due to the very high level of expression for GAS1 in luteal cells (Figs. 1E and 2B). By 72 h post-hCG, GAS1 remained detectable in most luteal cells (steroidogenic cells that emit autofluorescence), but the relative level of GAS1 expression in luteal cells versus stromal cells had decreased significantly (Fig. 2G). Taken together, GAS1 is expressed in ovarian stromal cells surrounding follicles and CL in a persistent and dynamic pattern.

Generation of Genetically Engineered Mice with Conditional Deletion of Gas1 *in Granulosa Cells and COCs*

GAS1 appears to regulate numerous cell processes that are context specific and signaling-pathway dependent [21]. Moreover, the *Gas1* knockout mice die shortly after birth [30]. Therefore, we sought to determine if selective depletion of *Gas1* in granulosa and cumulus cells would alter fertility and recapitulate any of the phenotypes of granulosa cells and COCs in *Cebpa/b*$^{fl/fl}$*;Cyp19a1-Cre* mutant mice. To accomplish this, we bred *Gas1*$^{fl/fl}$ mice to *Cyp19a1-Cre* mice to generate *Gas1*$^{fl/fl}$*;Cyp191a-Cre* mice [37] (Fig. 3A). Reduction and deletion of *Gas1* by *Cyp19a1-Cre* expression was confirmed using PCR of DNA extracted from granulosa cells and COCs from *Gas1*$^{fl/fl}$ controls, *Gas1*$^{fl/+}$*;Cyp191a-Cre,* and *Gas1*$^{fl/fl}$*;Cyp191a-Cre* mutant mice (Fig. 3B). *Gas1* was reduced in the granulosa cells of heterozygous mutant and absent in the homozygous mutant granulosa cells. In COCs, *Gas1* was expressed in heterozygous mutant and absent in homozygous mutant. Compared to *Gas1*$^{fl/fl}$ controls, GAS1 protein was not detected by IF staining in CL of *Gas1*$^{fl/fl}$*;Cyp191a-Cre* mutant mice at 24 and 48 h post-hCG (Fig. 3C), consistent with its absence in isolated CL from *Gas1* mutant females as detected using Western blot analyses (Fig. 3D).

Deletion of Gas1 *in Granulosa Cells and COCs Enhanced Ovulation Rates*

Fertility of female *Gas1*$^{fl/fl}$*;Cyp191a-Cre* mutant mice was tested by mating control and mutant females to proven fertile *Gas1*$^{fl/fl}$ males for 6 mo. The mutant females produced slightly, but not significantly, more pups than the *Gas1*$^{fl/fl}$ control mice throughout the 6-mo breeding assay (Fig. 4A). However, when stimulated with a superovulatory eCG/hCG treatment, *Gas1*$^{fl/fl}$*;Cyp191a-Cre* mutant females ovulated significantly more oocytes than the *Gas1*$^{fl/fl}$ control mice (Fig. 4B).

To analyze changes in the expression of selected genes in the *Gas1* mutant mice, we collected granulosa cells and COCs from *Gas1*$^{fl/fl}$*;Cyp191a-Cre* mutant mice and *Gas1*$^{fl/fl}$ control mice at 5 h post-hCG, a time interval when both C/EBPα and C/EBPβ protein levels were elevated and rapid changes in genes controlling ovulation are first observed. As expected, *Gas1* mRNA was significantly reduced in the *Gas1*$^{fl/fl}$*; Cyp191a-Cre* mutant mice compared to the *Gas1*$^{fl/fl}$ control mice in both granulosa cells and COCs. In these same granulosa cell samples, the expression of two genes, *Pgr* and *Ptgs2,* critical for ovulation did not change whereas mRNA levels of *Lhcgr* and *Areg* were significantly increased in the *Gas1*$^{fl/fl}$*;Cyp191a-Cre* mutant mice compared to controls (Fig. 4, C and D). The level of mRNA for *Areg* was also increased in COCs from the mutant mice compared to the controls (Fig. 4D). These differences in *Lhcgr* and *Areg* mRNA levels between wild-type and mutant mice were not detected before hCG stimulation (Fig. 5, A and B, 48 h post-eCG) or after

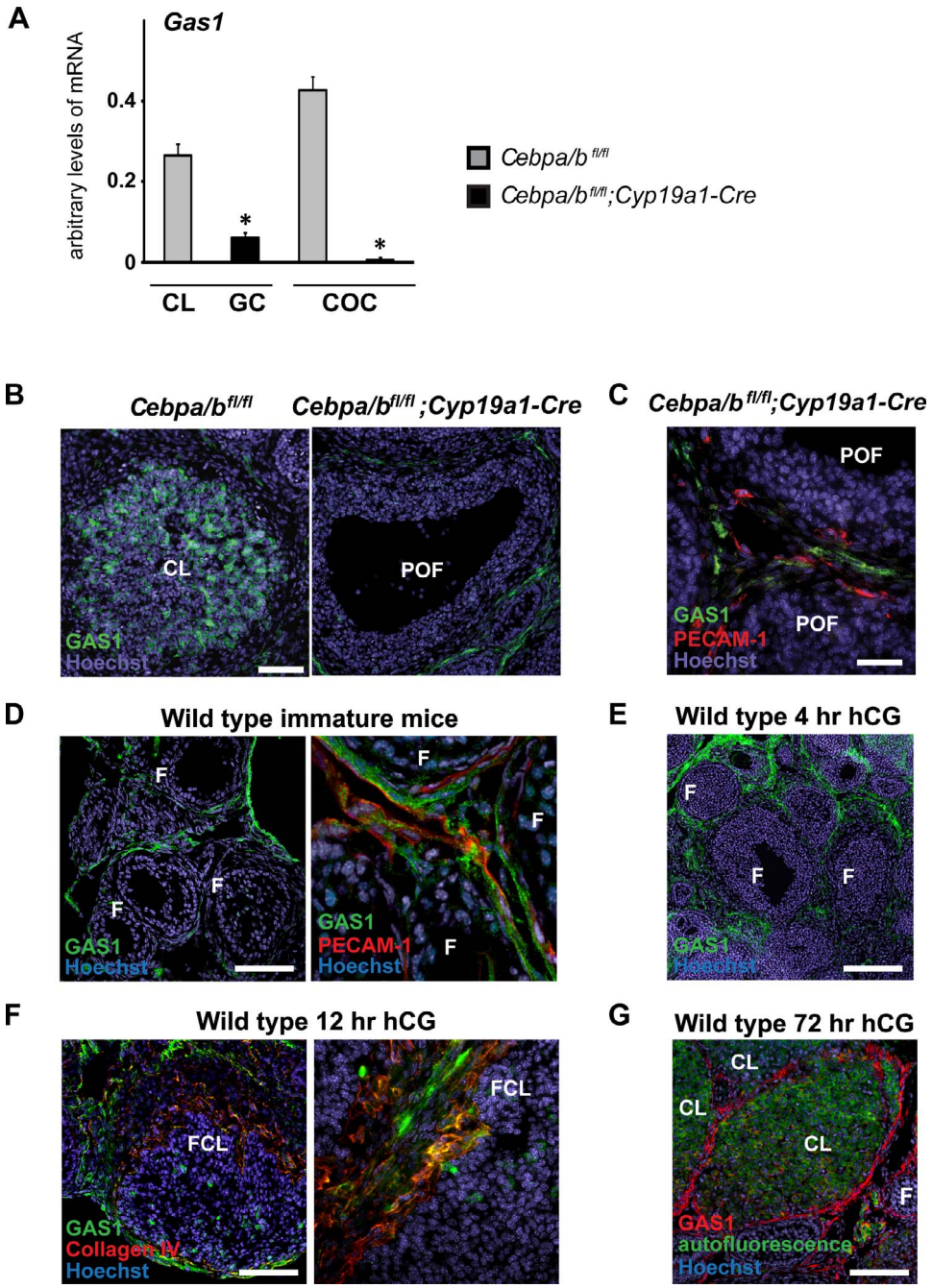

FIG. 2. Induction of *Gas1* expression in luteinizing granulosa cells depends on C/EBPα/β. **A**) Levels of *Gas1* mRNA in periovulatory granulosa cells (mutant mice) and luteinized granulosa cells (wild type) (24 h post-hCG) and COCs (16 h post-hCG) were significantly reduced in *Cebpa/b*$^{fl/fl}$*;Cyp19a1-Cre* mutant mice compared to wild-type controls. Data shows mean ± SEM; n = 3, *$P < 0.01$. **B**) Immunofluorescent localization of GAS1 in CL of wild-type controls and preovulatory follicles (POF) of *Cebpa/b*$^{fl/fl}$*;Cyp19a1-Cre* mutant mice at 16 h post-hCG. Bar = 50 μm. **C**) Immunofluorescent localization of GAS1 and PECAM-1 in POF of *Cebpa/b*$^{fl/fl}$*;Cyp19a1-Cre* mutant mice at 16 h post-hCG. Bar = 50 μm. **D**) Representative image of IF staining of GAS1 (green) or GAS1 and PECAM-1 (red) in ovaries of wild-type immature unstimulated mice. F, follicles. Bar = 100 (left) and 40 (right) μm. **E**) Representative image of IF staining of GAS1 (green) in ovaries at 4 h post-hCG stimulation. F, follicles. Bar = 200 μm. **F**) Representative image of IF staining of GAS1 (green) and collagen IV (red) in ovaries at 12 h post-hCG stimulation. FCL, forming corpus luteum. Bar = 100 (left) and 60 (right) μm. **G**) Representative image of IF staining of GAS1 and autofluorescent (green, from steroidogenic cells) signals in ovaries at 72 h post-hCG stimulation. F, follicles; CL, corpus luteum. Bar = 100 μm.

ovulation (Fig. 5, C and D, 16 h post-hCG). Together these observations suggest that the conditional deletion of *Gas1* in granulosa cells and COCs promotes ovulation and the expression of selected genes associated with ovulation.

Deletion of Gas1 *in Granulosa Cells Alters Expression of Key Genes in CL*

We next sought to determine if the depletion of *Gas1* in granulosa cells would also alter luteinization because 1) GAS1 mRNA and protein were maximally increased between 12–24

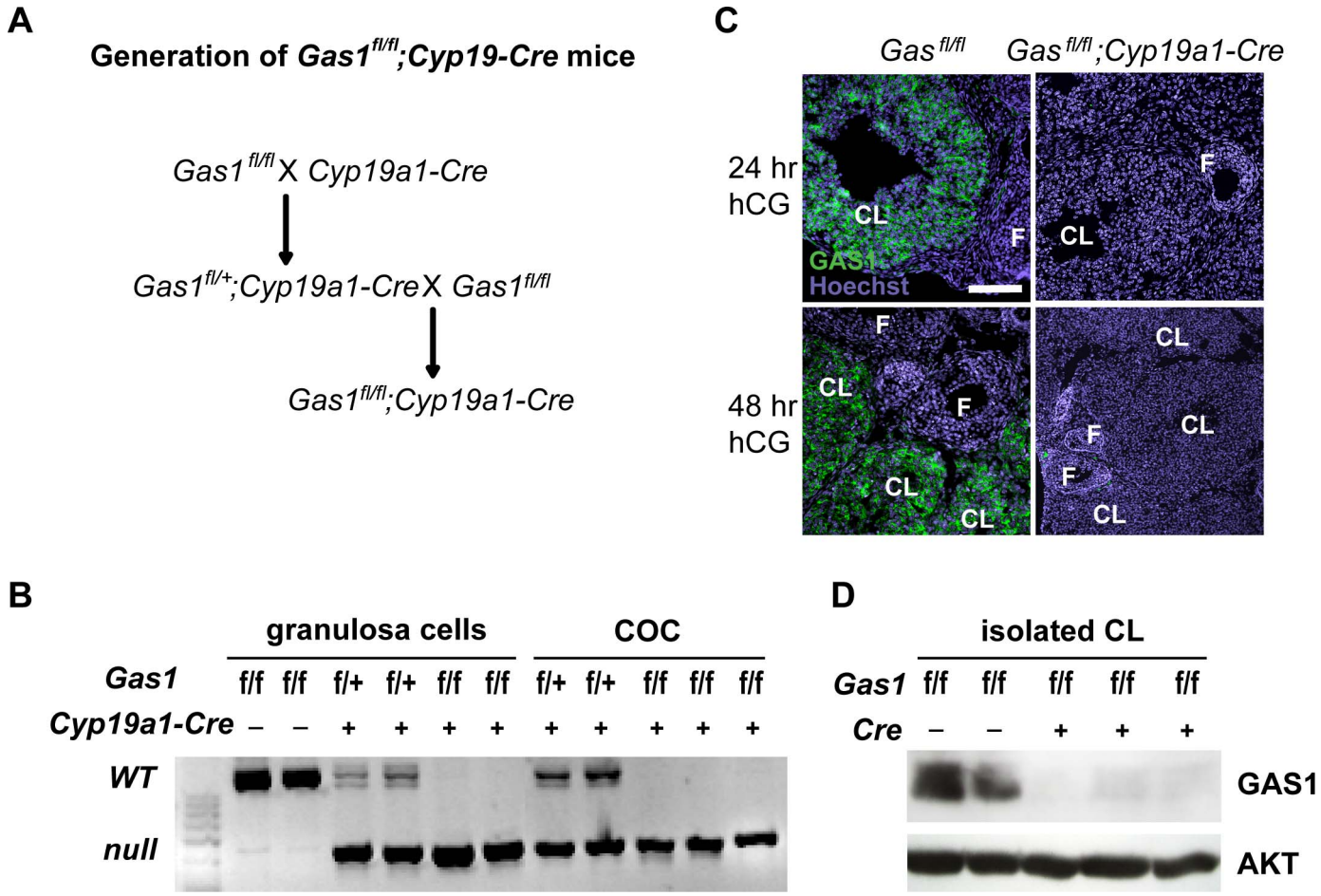

FIG. 3. Generation of mice with conditional deletion of *Gas1* in granulosa cells and COCs. **A**) Breeding scheme. **B**) PCR amplification of *Gas1* gene in wild-type, heterozygous, and homozygous *Gas1* mutant granulosa cells and COCs obtained at 24 h post-hCG. **C**) Immunofluorescent localization of GAS1 in ovaries of control and *Gas1*$^{fl/fl}$*;Cyp191a-Cre* mutant mice at 24 and 48 h post-hCG. F, follicles; CL, corpus luteum. Bar = 100 μm. **D**) Western blot analyses of GAS1 in isolated CL from *Gas1*$^{fl/fl}$ control and *Gas1*$^{fl/fl}$*;Cyp191a-Cre* mutant adult female mice. Each sample represents CL isolated from an individual mouse.

h post-hCG, 2) *Gas1* is a target of C/EBPα/β and appears to be selectively increased during luteinization when granulosa cells cease dividing and become terminally differentiated, and 3) GAS1 has been reported to be a regulator of proliferation and differentiation [29, 43]. We first confirmed the reduced expression of *Gas1* in whole ovaries of the *Gas1*$^{fl/fl}$*;Cyp191a-Cre* mutant mice at 24 and 48 h post-hCG (Fig. 6, A and B, left). In addition, the expression of several luteinization-related genes was reduced in the *Gas1* mutant ovaries compared to *Gas1*$^{fl/fl}$ control mice at 24 h post-hCG (Fig. 6A). These included genes involved in luteinization (*Prlr*), steroidogenesis (*Star* and *Cyp11a1*), WNT signaling (*Wnt4*), angiogenesis (*Sema3a*), and cumulus/immune cell functions (*Cd52*) [44, 45]. Cell cycle-related genes (*Ccnd1, Ccnd2, Cdkn1a,* and *Cdkn1b*) were not altered (Fig. 6A; data not shown for *Ccnd2*). Importantly, most of these luteinization-related genes are also targets of C/EBPα/β, supporting the observations that *Gas1* mediates some processes associated with luteinization and that are downstream of C/EBPα/β [10]. Interestingly, by 48 h post-hCG, differences in mRNA levels of the above-mentioned luteal genes in ovarian samples were no longer detectable, with the exception of *Cdkn1b* that was reduced (but not statistically significant) (Fig. 6B). Because compensation from redundant mechanisms or pathways may rescue phenotypes caused by in vivo deletion of *Gas1*, we next tested whether acute in vitro deletion could cause similar effects by exposing *Gas1*$^{fl/fl}$ granulosa cells to *Cre*-expressing adenovirus (Fig. 6C). Fo/PMA treatment of granulosa cells collected from eCG-primed immature mice (24 h post-eCG) induced elevated mRNA expression of key genes in CL (*Sema3a, Wnt4, Prlr, Cd52, Star,* and *Cyp11a1*) at 24 h of treatment as expected whereas depletion of *Gas1* using *Cre*-expressing adenovirus efficiently suppressed induction of *Gas1* expression (data not shown) as well as significantly dampened the induction of *Sema3a, Prlr, Cd52,* and *Star*. In vitro depletion of *Gas1* also reduced expression of *Wnt4* and *Cyp11a1,* but the reduction was not statistically significant. Thus, depletion of *Gas1* does impact induction of selected luteal cell genes during the initial stages of luteinization.

Disruption of the Gas1 *in Granulosa Cells Does Not Impair CL Vascularization*

Based on the reduced mRNA levels of critical luteal cell steroidogenic genes *Cyp11a1* and *Star* in *Gas1*$^{fl/fl}$*;Cyp191a-Cre* mutant mice compared to controls, we hypothesized that the serum progesterone levels might also be reduced in these mutant mice. However, this was not the case (Fig. 7A). The gross histological appearance of CL was also comparable between the mutant and control ovaries (Fig. 7B). Because the circulating levels of progesterone are determined not only

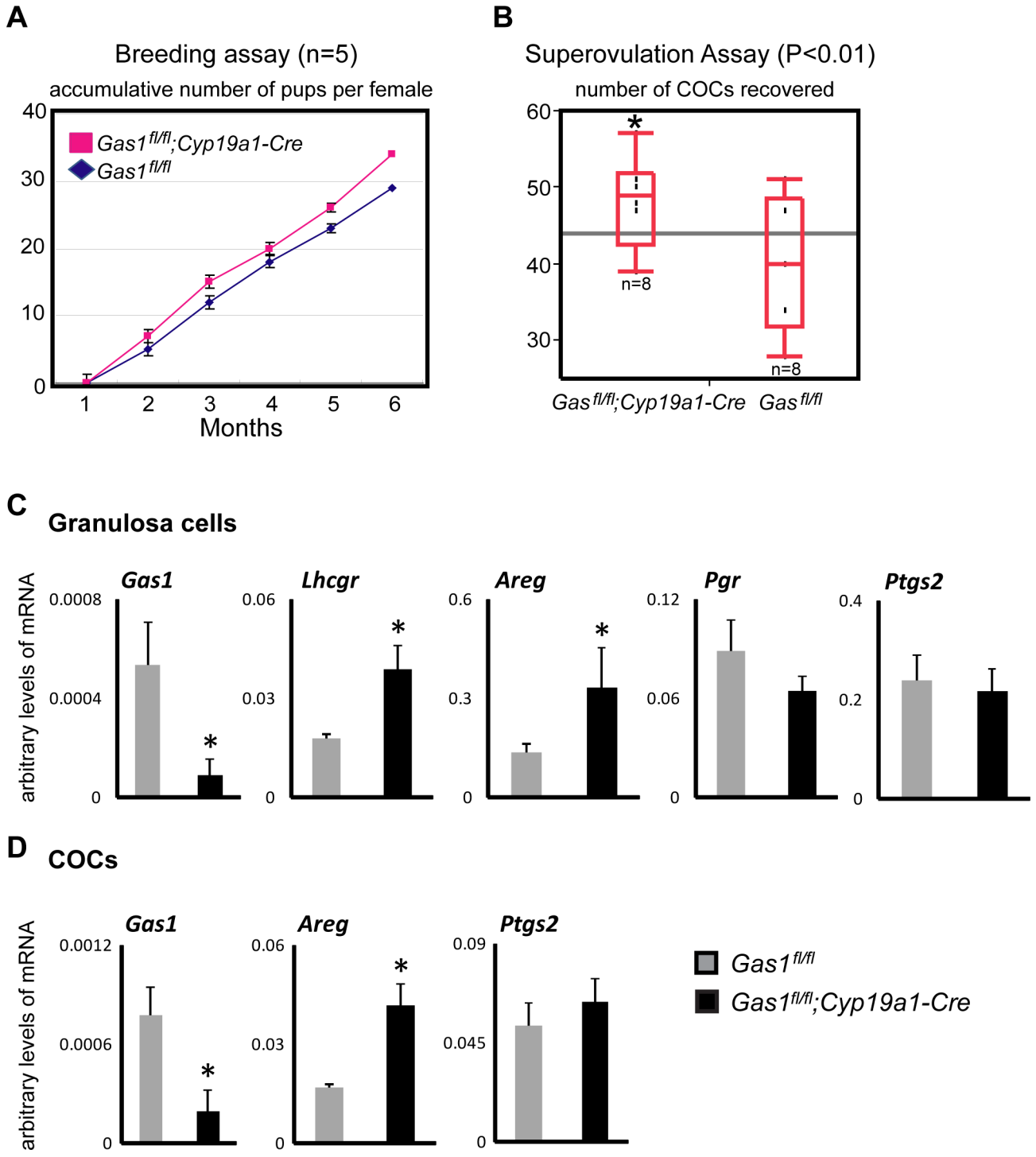

FIG. 4. Conditional deletion of *Gas1* in granulosa cells and COCs promotes ovulation. **A**) Breeding assay of *Gas1*$^{fl/fl}$*;Cyp191a-Cre* mutant mice and *Gas1*$^{fl/fl}$ controls; n = 5. **B**) Superovulation studies of *Gas1*$^{fl/fl}$*;Cyp191a-Cre* mutant mice and *Gas1*$^{fl/fl}$ controls; n = 8, *$P < 0.01$. **C**) Levels of mRNA for *Gas1* and ovulation/luteinization-associated genes in granulosa cells from *Gas1*$^{fl/fl}$*;Cyp191a-Cre* mutant mice and wild-type controls at 5 h post-hCG. Data shows mean ± SEM; n = 4, *$P < 0.05$. **D**) Levels of mRNA for *Gas1* and ovulation-associated genes in COCs from *Gas1*$^{fl/fl}$*;Cyp191a-Cre* mutant mice and wild-type controls at 5 h post-hCG. Data shows mean ± SEM; n = 4, *$P < 0.05$.

by its synthesis and secretion, but also by its transportation from CL to the circulation via the luteal vasculature, we investigated whether there was enhanced vasculature in the CL of *Gas1*$^{fl/fl}$*;Cyp191a-Cre* mutant mice (Fig. 7C). Immunofluorescent staining confirmed the depletion of GAS1 protein in CL of the *Gas1*$^{fl/fl}$*;Cyp191a-Cre* mutant mice, but staining with vascular markers collagen IV and PECAM-1 demonstrated similar temporal and spatial vascularization processes in the CL of *Gas1* mutant and wild-type control ovaries. At 24 h post-hCG, deposits of collagen IV were visible throughout the newly FCL, and endothelial cells (PECAM-1 positive) were branching in between luteinizing granulosa cells in both *Gas1* mutant and wild-type control ovaries. Furthermore, a closer look revealed that GAS1

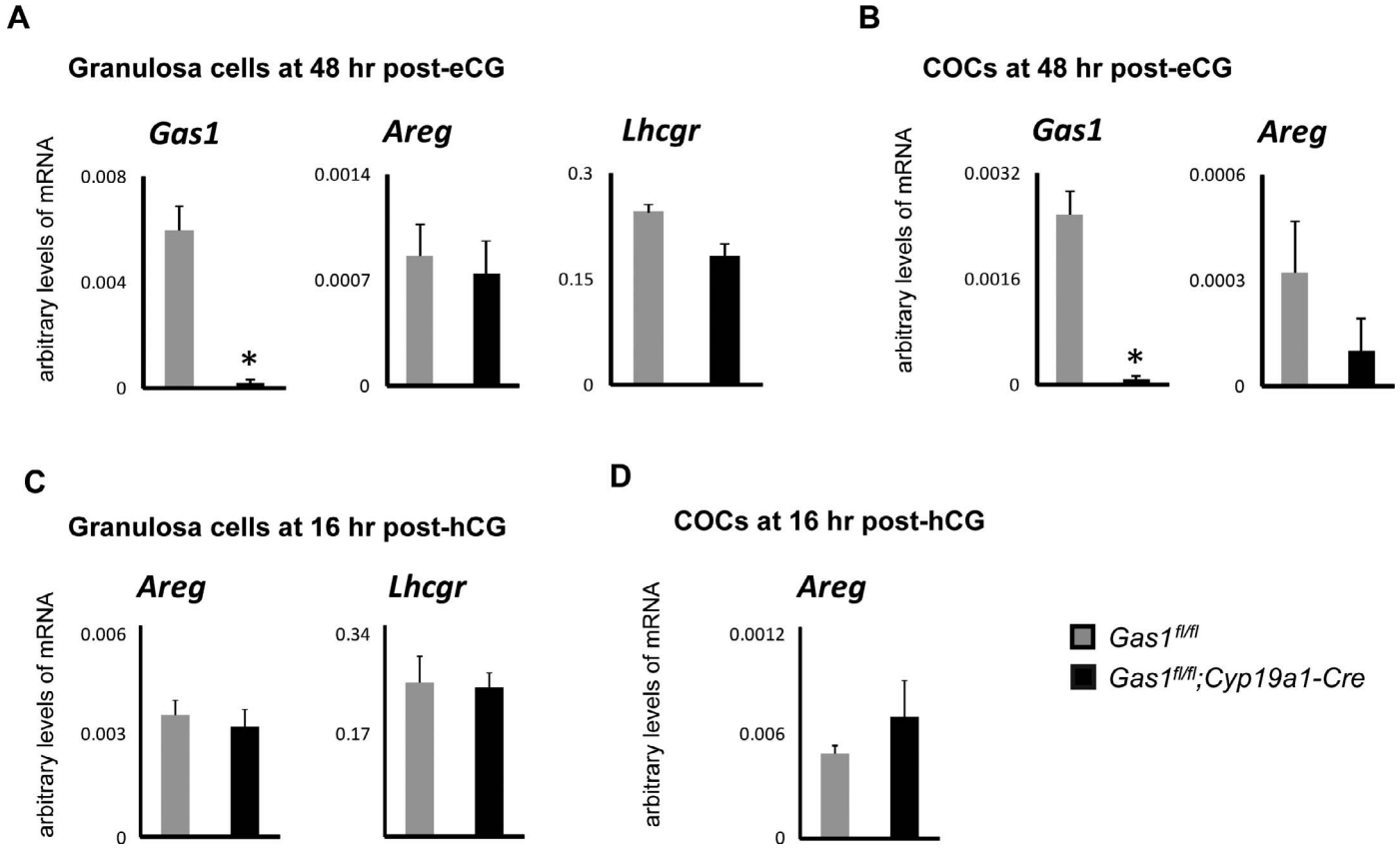

FIG. 5. Levels of mRNA for *Areg* and *Lhcgr* were not altered in granulosa cells or COCs of *Gas1*$^{fl/fl}$*;Cyp191a-Cre* mutant mice compared to controls before hCG stimulation (**A** and **B**) (48 h post-eCG) or after ovulation (**C** and **D**) (16 h post-hCG). Data shows mean ± SEM; n = 3, *$P < 0.05$.

colocalized with some collagen IV in the newly FCL but not with PECAM-1 (Fig. 7D), indicating that GAS1 is selectively expressed in luteinizing granulosa cells and not endothelial cells during the neovascularization processes after ovulation.

DISCUSSION

The glycosyl phosphatidylinositol-linked GAS1 protein appears to have specific functions in many tissues at different stages of development [29]. These include cell cycle arrest, apoptosis, morphogenesis, and differentiation [26, 46, 47]. These diverse functions of GAS1 may be related to tissue-specific transcription factors that can activate the *Gas1* gene (such as p53) [22, 48] as well as to diverse signaling pathways (including WNT, HH, and GDNF) with which GAS1 is known to interact [29].

Our studies on the expression and function of GAS1 in ovarian follicles provide additional, novel evidence that 1) the expression of the *Gas1* gene is dependent, at least in part, on the C/EBPα/β transcription factors as revealed by its impaired expression in granulosa, cumulus, and luteal cells of the *Cebpa/b*$^{fl/fl}$*;Cyp19a1-Cre* mice (Fig. 2) and 2) GAS1 protein localizes to granulosa, cumulus, and luteal cells and impacts the expression of specific genes involved in ovulation and the initiation of luteinization (Fig. 5). Specifically, we show that GAS1 mRNA and protein are low in granulosa cells of pre-ovulatory follicles but are selectively increased in granulosa and cumulus cells of ovulating follicles following LH/hCG, and in luteal cells of newly FCL, suggesting its involvement in ovulation and early-stage CL function.

The physiological relevance to and impact of GAS1 in ovulation is clearly demonstrated by the increased the rate of ovulation in the *Gas1* conditional knockout mice during normal breeding and, more dramatically, in response to exogenous gonadotropins. Moreover, *Gas1* depletion in granulosa cells in vivo leads to the increased expression of the LH receptor (*Lhcgr*) and the EGF-like factor *Areg* in the granulosa cells and cumulus cell in vivo, both of which are known to be essential for ovulation and luteinization [7, 49]. Because GAS1 protein levels are low in granulosa cells of preovulatory follicles, these results suggest that GAS1, even at low levels of expression, may suppress the responsiveness of granulosa cells to signals that both promote preovulatory follicular development and ovulation. The mechanisms that mediate the effect of GAS1 on follicular development and ovulation are not clear, but based on the cytoplasmic/membrane localization of GAS1, it may directly or indirectly interact with the LH receptor or other membrane-related factors. After hCG stimulation and especially in the immediate postovulatory period (12–16 h post-hCG), expression of GAS1 was dramatically induced in both luteinizing granulosa cells and COCs, a time point corresponding to a further increase in the protein level of C/EBPβ at 12–16 h post-hCG [50], and presumably a time when C/EBPα/β bind to the promoter of the *Gas1* gene and directly regulate its transcription in the ovary, inducing *Gas1* mRNA expression in both granulosa cells and COCs. Because AREG is transiently induced during ovulation and the LHCGR is down-regulated following the LH surge, the rapid induction of GAS1 may also act to prevent prolonged expression of AREG and LHCGR that would be predicted to alter the ovulation and luteinization processes.

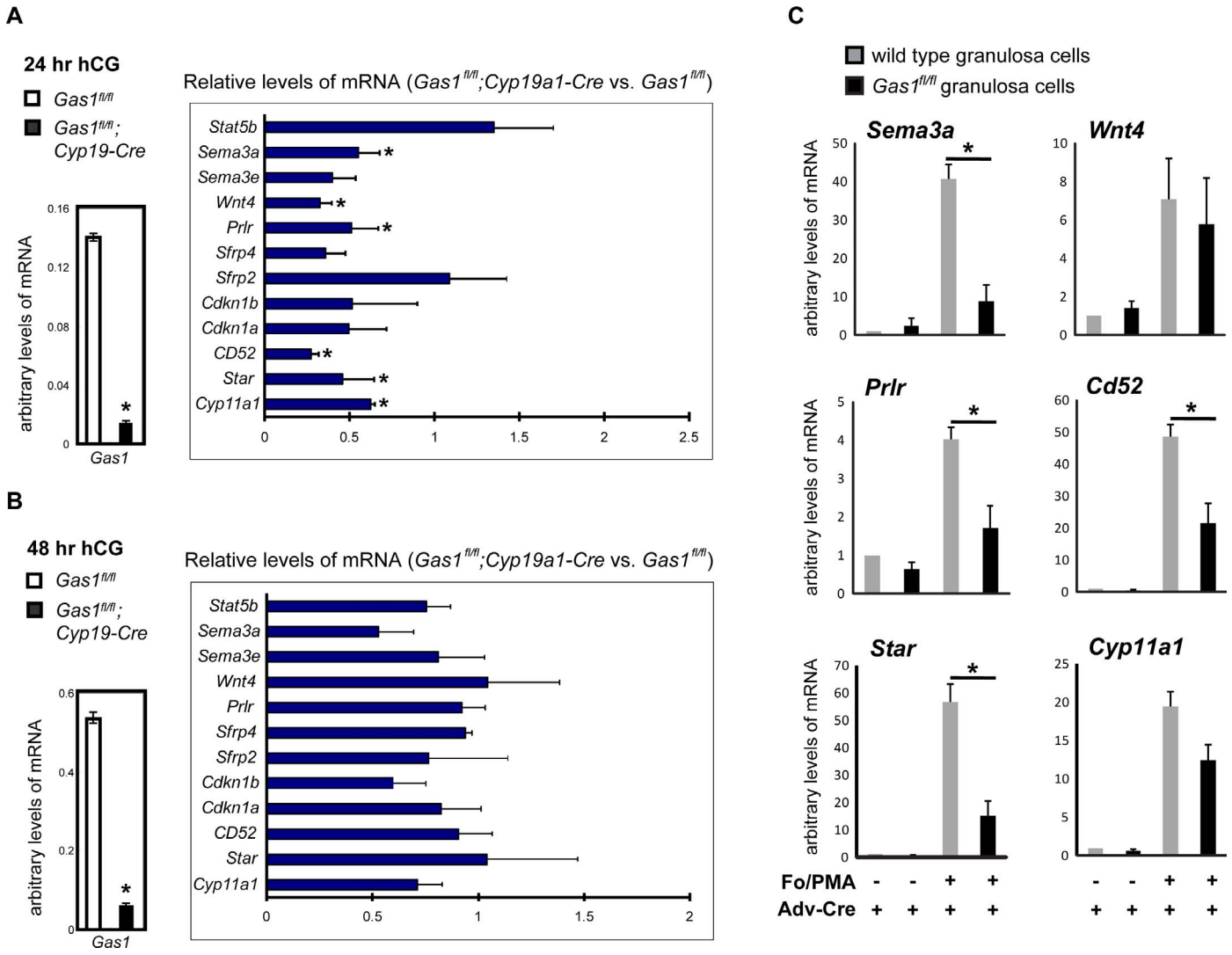

FIG. 6. Levels of mRNA for key genes in CL were altered in *Gas1*$^{fl/fl}$*;Cyp191a-Cre* mutant mice compared to controls. **A**) Levels of mRNA for *Gas1* and luteal genes in whole ovaries from *Gas1* mutant and control mice at 24 h post-hCG. Data for luteal genes are presented as the relative values in the mutants divided by those in controls; n = 4, *$P < 0.05$. **B**) The mRNA of *Gas1* and luteal genes in whole ovaries of *Gas1* mutant and control mice at 24 h post-hCG. Data for luteal genes are presented as the relative values in the mutants divided by those in controls; n = 5, *$P < 0.05$. **C**) Deletion of Gas1 in vitro in cultured granulosa cells reduced mRNA levels of luteal genes. Fo/PMA treatment was given for 24 h.

The physiological relevance of GAS1 to luteal cell function and the formation of the CL is shown by its elevated expression and localization to luteal cells 24 h post-hCG and to the impaired expression of specific genes during the initial phase of luteinization. Specifically, once the ovulation and luteinization programs have been set in motion by the LH surge, GAS1 increases markedly and appears to be a downstream target of C/EBPα/β [18, 19]. Genes with altered mRNA levels in the CL of *Gas1*$^{fl/fl}$*;Cyp191a-Cre* mice, such as *Sema3a, Cyp11a1, Star, Prlr,* and *Wnt4,* are also targets of C/EBPβ, thus supporting GAS1 as a mediator of at least some effects of C/EBPβ on the luteinization process. Disruption of *Gas1* expression in cultured granulosa cells with adenoviral-Cre further confirms a role for GAS1 in regulating these luteal-related genes as well as the immune-related gene *Cd52* [51]. Although a plethora of data demonstrate that two major functions of GAS1 are to cause cell cycle arrest and apoptosis [24, 43, 46], disruption of the *Gas1* gene in granulosa cells does not impair granulosa cell cycle arrest or prevent their terminal differentiation to nondividing luteal cells in response to LH/hCG. This could be dependent, in part, on the degree of *Gas1* depletion in granulosa cells because our data show that even low levels of *Gas1* mRNA and protein appear critical for regulating induction of genes such as *Areg*. Additionally, the effects of GAS1 are likely context specific and related to in vivo versus in vitro analyses, the cell type being analyzed (NIH-3T3 and COMMA D cells, adipocytes, or endothelial cells), the isoforms of C/EBP present or other transcription factors being expressed, and the cell-type-specific pathways that are coordinately activated.

GAS1 exerts a myriad of functions through its interactions with multiple pathways during development, including the HH-, WNT-, and GDNF/RET-signaling pathways. However, although GAS1 can interact with the G-protein-coupled HH-signaling receptor SMO and well as CDO and BOC [28, 52–54], the HH-signaling pathway is suppressed to a minimal level in granulosa cells after LH surge [55, 56]. Thus, it is unlikely that the HH-signaling pathway is a key interacting factor with GAS1 in the preovulatory follicles and CL. However, it is possible that ovarian stromal cell GAS1 may interact with the HH-signaling pathway to impact early stages of follicular development, perhaps by regulating differentia-

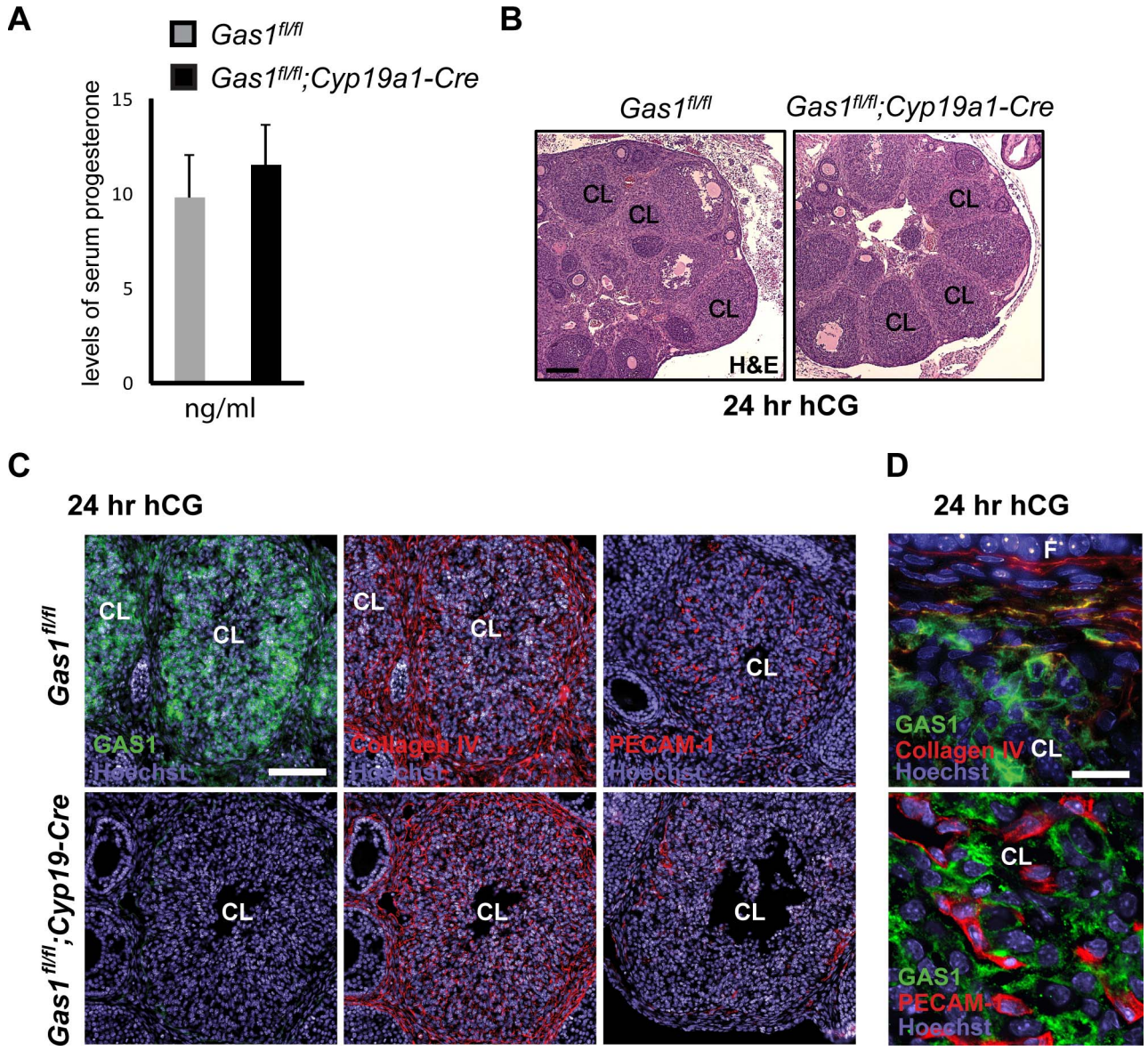

FIG. 7. GAS1 does not directly regulate vascular development in CL. **A**) Serum levels of progesterone in *Gas1* mutant and control mice at 24 h post-hCG. Data represents mean ± SEM, n = 5. **B**) Representative images of H&E staining on ovarian sections from *Gas1* mutant and control mice at 24 h post-hCG. Bar = 100 μm. **C**) Representative images of IF staining of GAS1, collagen IV, and PECAM-1 on ovarian sections from *Gas1* mutant and control mice. Bar = 100 μm. **D**) Representative images of IF localization of GAS1, collagen IV, and PECAM-1 on wild-type ovarian sections. Bar = 10 μm. CL, corpus luteum.

tion of α-smooth muscle actin-positive cells. The transient impact of GAS1 depletion in the newly FCL on the other hand, is likely to be partially through other G-protein-coupled receptors, such as the LH receptor itself or the WNT/FZD-signaling pathway, both of which play key roles in the formation and function of CL [42, 57–60], including regulation of the expression of steroidogenesis genes *Cyp11a1*, *Star*, and *Cyp19a1*, as well as CL vascularization [10].

Although a previous study reported that GAS1 is regulated by VE-cadherin and VEGF in endothelial cells [32], this does not seem to be the case in growing follicles or CL because GAS1 does not colocalize or exhibit close proximity with the endothelial marker PECAM-1. Expression of GAS1 in CL appears to be specific for luteal cells because it colocalized with SFRP4, a known marker for luteal cells, and because GAS1 was no longer detectable using IF staining when depleted with granulosa cell/luteal cell-specific *Cyp19a1-Cre*. Moreover, different from SFRP4, which is a secreted protein and can exhibit diffusive localization and is even detected in serum, the distinct membrane localization of GAS1 makes it an easily identifiable new marker for luteal cells as compared to granulosa cells.

In summary, based on the rapid induction but transient expression of GAS1 in ovulating follicles and CL and the impact of its depletion in granulosa, cumulus, and luteal cells, GAS1 is a C/EBP-target gene that is involved in follicular development, ovulation, and luteinization. The granulosa cell-specific depletion of *Gas1* enhanced the rate of ovulation both in regular breeding assays and upon superovulatory hormone stimulation, and this was associated with enhanced expression of *Areg* and *Lhcgr*, key factors known to mediate preovulatory follicle responses to the LH surge [7, 61]. Conversely, depletion of *Gas1* reduced the expression of luteal cell-related genes, suggesting that it may also impact luteal cell functions.

ACKNOWLEDGMENT

The authors thank Dr. Victor Kostyuk for statistical analyses.

REFERENCES

1. Richards JS. Hormonal control of ovarian follicular development: a 1978 perspective. Recent Prog Hormone Res 1979; 35:343–373.
2. Richards JS, Pangas SA. The ovary: basic biology and clinical implications. J Clin Invest 2010; 120:963–972.
3. Fan HY, Liu Z, Shimada M, Sterneck E, Johnson PF, Hedrick SM, Richards JS. MAPK3/1 (ERK1/2) in ovarian granulosa cells are essential for female fertility. Science 2009; 324:938–941.
4. Hsieh M, Conti M. G-protein-coupled receptor signaling and the EGF network in endocrine systems. Trends Endocrinol Metab 2005; 16: 3320–3326.
5. Hsieh M, Lee D, Panigone S, Horner K, Chen R, Theologis A, Lee DC, Threadgill DW, Conti M. Luteinizing hormone-dependent activation of the epidermal growth factor network is essential for ovulation. Mol Cell Biol 2007; 27:1914–1924.
6. Conti M, Hsieh M, Park J-Y, Su Y-Q. Role of the EGF network in ovarian follicles. Mol Endocrinol 2005; 20:715–723.
7. Park JY, Su YQ, Ariga M, Law E, Jin SL, Conti M. EGF-like growth factors as mediators of LH action in the ovulatory follicle. Science 2004; 303:682–684.
8. Shimada M, Gonzalez-Robayna I, Hernandez-Gonzalez I, Richards JS. Paracrine and autocrine regulation of EGF-like factors in cumulus oocyte complexes and granulosa cells: key role for prostaglandin synthase 2 (*Ptgs2*) and progesterone receptor (*Pgr*). Mol Endocrinol 2006; 20: 348–364.
9. Sterneck E, Tassarollo L, Johnson PF. An essential role for C/EBPb in female reproduction. Genes Dev 1997; 11:2153–2162.
10. Fan HY, Liu Z, Johnson PF, Richards JS. CCAAT/enhancer-binding proteins (C/EBP)-alpha and -beta are essential for ovulation, luteinization, and the expression of key target genes. Mol Endocrinol 2011; 25:253–268.
11. Poli V. The role of C/EBP isoforms in the control of inflammatory and native immunity functions. J Biol Chem 1999; 273:29279–29282.
12. Rahman SM, Janssen RC, Choudhury M, Baquero KC, Aikens RM, de la Houssaye BA, Friedman JE. CCAAT/enhancer-binding protein β (C/EBPβ) expression regulates dietary-induced inflammation in macrophages and adipose tissue in mice. J Biol Chem 2012; 287:34349–34360.
13. Rosen ED, MacDougald OA. Adipocyte differentiation from the inside out. Nat Rev Mol Cell Biol 2006; 7:885–896.
14. Mantena SR, Kannan A, Cheon Y-P, Li Q, Johnson PF, Bagchi IC, Bagchi MK. C/EBPb is a critical mediator of steroid hormone-regulated cell proliferation and differentiation in the uterine epithelium and stroma. Proc Natl Acad Sci U S A 2006; 103:1870–1875.
15. Ramanthal C, Bagchi IC, Bagchi MK. Lack of CCAAT enhancer binding protein beta (C/EBPb) in uterine epithelial cells impairs estrogen-induced DNA replication, induces DNA damage response pathways, and promotes apoptosis. Mol Cell Biol 2010; 30:1607–1619.
16. Sirois J, Richards JS. Transcriptional regulation of the rat prostaglandin endoperoxide synthase 2 gene in granulosa cells. Evidence for a role of a cis acting C/EBP beta promoter element. J Biol Chem 1993; 268: 21931–21938.
17. Burkart AD, Mukherjee A, Sterneck E, Johnson PF, Mayo KE. Repression of the inhibin alpha-subunit gene by the transcription factor CCAAT/enhancer-binding protein-beta. Endocrinology 2005; 146:1909–1921.
18. Lefterova MI, Zhang Y, Steger DJ, Schupp M, Schug J, Cristancho A, Feng D, Zhuo D, Stoeckert CJ Jr, Liu XS, Lazar MA. PPARgamma and C/EBP factors orchestrate adipocyte biology via adjacent binding on a genome-wide scale. Genes Dev 2008; 22:2941–2952.
19. Grontved L, John S, Baek S, Liu Y, Buckley JR, Vinson C, Aguilera G, Hager GL. C/EBP maintains chromatin accessibility in liver and facilitates glucocorticoid receptor recruitment to steroid response elements. EMBO J 2013; 32:1568–1583.
20. Evdokiou A, Cowled PA. Growth-regulatory activity of the growth arrest-specific gene, GAS1, in NIH3T3 fibroblasts. Exp Cell Res 1998; 240: 359–367.
21. Martinelli DC, Fan CM. The role of Gas1 in embryonic development and its implications for human disease. Cell Cycle 2007; 6:2650–2655.
22. Benitez JA, Arregui L, Vergara P, Segovia J. Targeted-simultaneous expression of Gas1 and p53 using a bicistronic adenoviral vector in gliomas. Cancer Gene Therapy 2007; 14:836–846.
23. Evdokiou A, Cowled PA. Tumor-suppressive activity of the growth arrest-specific gene GAS1 in human tumor cell lines. Int J Cancer 1998; 75: 568–577.
24. Gobeil S, Zhu X, Doillon CJ, Green MR. A genome-wide shRNA screen identifies GAS1 as a novel melanoma metastasis suppressor gene. Genes Dev 2008; 22:2932–2940.
25. Lee CS, May NR, Fan C-M. Transdifferentiation of the ventral retinal pigmented epithelium to neural retina in the growth arrest specific gene 1 mutant. Dev Biol 2001; 236:17–29.
26. Seppala M, Depew MJ, Martinelli DC, Fan C-M, Sharpe PT, Cobourne MT. Gas1 is a modifier for holoprosencephaly and genetically interacts with sonic hedgehog. J Clin Investig 2007; 117:1575–1584.
27. Biau S, Jin S, Fan C-M. Gastrointestinal defects of the Gas1 mutant involve dysregulated Hedgehog and Ret signaling. Biol Open 2013; 2: 144–155.
28. Allen BL, Tenzen T, McMahon AP. The Hedgehog-binding proteins Gas1 and Cdo cooperate to positively regulate Shh signaling during mouse development. Genes Dev 2007; 21:1244–1257.
29. Martinelli DC, Fan C-M. Gas1 extends the range of Hedgehog action by facilitating its signaling. Genes Dev 2007; 21:1231–1243.
30. Lee CS, Buttitta L, Fan CM. Evidence that the WNT-inducible growth arrest-specific gene 1 encodes an antagonist of sonic hedgehog signaling in the somite. Proc Natl Acad Sci U S A 2001; 98:11347–11352.
31. Cabrera JR, Sanchez-Pulido L, Rojas AM, Valencia A, Mañes S, Naranjo JR, Mellström B. Gas1 is related to the glial cell-derived neurotrophic factor family receptors α and regulates ret signaling. J Biol Chem 2006; 281:14330–14339.
32. Spagnuolo R, Corada M, Orsenigo F, Zanetta L, Deuschle U, Sandy P, Schneider C, Drake CJ, Breviario F, Dejana E. Gas1 is induced by VE-cadherin and vascular endothelial growth factor and inhibits endothelial cell apoptosis. Blood 2004; 103:3005–3012.
33. Leem Y-E, Han J-W, Lee H-J, Ha H-L, Kwon Y-L, Ho S-M, Kim B-G, Tran P, Bae G-U, Kang J-S. Gas1 cooperates with Cdo and promotes myogenic differentiation via activation of p38MAPK. Cell Signal 2011; 23:2021–2029.
34. Lefterova MI, Zhang Y, Steger DJ, Schupp M, Schug J, Cristancho A, Feng D, Zhuo D, Stoeckert CJ, Liu XS, Lazar MA. PPARγ and C/EBP factors orchestrate adipocyte biology via adjacent binding on a genome-wide scale. Genes Dev 2008; 22:2941–2952.
35. Grontved L, John S, Baek S, Liu Y, Buckley JR, Vinson C, Aguilera G, Hager GL. C/EBP maintains chromatin accessibility in liver and facilitates glucocorticoid receptor recruitment to steroid response elements. EMBO J 2013; 32:1568–1583.
36. Guo K, Wolf V, Dharmarajan AM, Feng Z, Bielke W, Saurer S, Friis R. Apoptosis-associated gene expression in the corpus luteum of the rat. Biol Reprod 1998; 58:739–746.
37. Jin S, Martinelli DC, Zheng X, Tessier-Lavigne M, Fan CM. Gas1 is a receptor for sonic hedgehog to repel enteric axons. Proc Natl Acad Sci U S A 2015; 112:E73–E80.
38. Fan HY, Shimada M, Liu Z, Cahill N, Noma N, Wu Y, Gossen J, Richards JS. Selective expression of KrasG12D in granulosa cells of the mouse ovary causes defects in follicular development and ovulation. Development 2008; 135:2127–2137.
39. Liu Z, Castrillon DH, Zhou W, Richards JS. FOXO1/3 depletion in granulosa cells alters follicle growth, death and regulation of pituitary FSH. Mol Endocrinol 2013; 27:238–252.
40. Varani S, Elvin JA, Yan C, DeMayo J, DeMayo FJ, Horton HF, Byrne MC, Matzuk MM. Knockout of pentraxin 3, a downstream target of growth differentiation factor-9, causes female subfertility. Mol Endocrinol 2002; 16:1154–1167.
41. Nautiyal J, Steel JH, Rosell MM, Nikolopoulou E, Lee K, Demayo FJ, White R, Richards JS, Parker MG. The nuclear receptor cofactor receptor-interacting protein 140 is a positive regulator of amphiregulin expression and cumulus cell-oocyte complex expansion in the mouse ovary. Endocrinology 2010; 151:2923–2932.
42. Hsieh M, Boerboom D, Shimada M, Lo Y, Parlow AF, Luhmann UF, Berger W, Richards JS. Mice null for Frizzled4 (Fzd4-/-) are infertile and exhibit impaired corpora lutea formation and function. Biol Reprod 2005; 73:1135–1146.
43. Del Sal G, Ruaro ME, Philipson L, Schneider C. The growth arrest-specific gene, gas1, is involved in growth suppression. Cell 1992; 70: 595–607P. MID:1505026.
44. Hasegawa A, Takenobu T, Kasumi H, Komori S, Koyama K. CD52 is synthesized in cumulus cells and secreted into the cumulus matrix during ovulation. Am J Reprod Immunol 2008; 60:187–191.
45. Koyama K, Hasegawa A, Komori S. Functional aspects of CD52 in reproduction. J Reprod Immunol 2009; 83:56–59.
46. Zarco N, González-Ramírez R, González R, Segovia J. GAS1 induces cell death through an intrinsic apoptotic pathway. Apoptosis 2012; 17: 627–635.

47. Ma Y, Qin H, Cui Y. MiR-34a targets GAS1 to promote cell proliferation and inhibit apoptosis in papillary thyroid carcinoma via PI3K/Akt/Bad pathway. Biochem Biophys Res Commun 2013; 441:958–963.
48. Quante T, Otto B, Brázdová M, Kejnovská I, Deppert W, Tolstonog GV. Mutant p53 is a transcriptional co-factor that binds to G-rich regulatory regions of active genes and generates transcriptional plasticity. Cell Cycle 2012; 11:3290–3303.
49. Richards JS. Genetics of ovulation. Semin Reprod Med 2007; 25: 235–242.
50. Fan HY, Liu Z, Shimada M, Sterneck E, Johnson PF, Hedrick SM, Richards JS. MAPK3/1 (ERK1/2) in ovarian granulosa cells are essential for female fertility. Science 2009; 324:938–941.
51. Shimada M, Hernandez-Gonzalez I, Gonzalez-Robayna I, Richards JS. Paracrine and autocrine regulation of epidermal growth factor-like factors in cumulus oocyte complexes and granulosa cells: key roles for prostaglandin synthase 2 and progesterone receptor. Mol Endocrinol 2006; 20:1352–1365.
52. Izzi L, Levesque M, Morin S, Laniel D, Wilkes BC, Mille F, Krauss RS, McMahon AP, Allen BL, Charron F. Boc and Gas1 each form distinct Shh receptor complexes with Ptch1 and are required for Shh-mediated cell proliferation. Dev Cell 2011; 20:788–801.
53. Leem YE, Han JW, Lee HJ, Ha HL, Kwon YL, Ho SM, Kim BG, Tran P, Bae GU, Kang JS. Gas1 cooperates with Cdo and promotes myogenic differentiation via activation of p38MAPK. Cell Signal 2011; 23: 2021–2029.
54. Allen BL, Song JY, Izzi L, Althaus IW, Kang JS, Charron F, Krauss RS, McMahon AP. Overlapping roles and collective requirement for the coreceptors GAS1, CDO, and BOC in SHH pathway function. Dev Cell 2011; 20:775–787.
55. Wijgerde M, Ooms M, Hoogerbrugge JW, Grootegoed JA. Hedgehog signaling in mouse ovary: Indian hedgehog and desert hedgehog from granulosa cells induce target gene expression in developing theca cells. Endocrinology 2005; 146:3558–3566.
56. Ren Y, Cowan RG, Harman RM, Quirk SM. Dominant activation of the hedgehog signaling pathway in the ovary alters theca development and prevents ovulation. Mol Endocrinol 2009; 23:711–723.
57. Lapointe E, Boyer A, Rico C, Paquet M, Franco HL, Gossen J, DeMayo FJ, Richards JS, Boerboom D. FZD1 regulates cumulus expansion genes and is required for normal female fertility in mice. Biol Reprod 2012; 87: 104.
58. Pan H, Cui H, Liu S, Qian Y, Wu H, Li L, Guan Y, Guan X, Zhang L, Fan HY, Ma Y, Li R, et al. Lgr4 gene regulates corpus luteum maturation through modulation of the WNT-mediated EGFR-ERK signaling pathway. Endocrinology 2014; 155:3624–3637.
59. Kendall SK, Samuelson LC, Saunders TL, Wood RI, Camper SA. Targeted disruption of the pituitary glycoprotein hormone alpha-subunit produces hypogonadal and hypothyroid mice. Genes Dev 1995; 9: 2007–2019.
60. Ma X, Dong Y, Matzuk MM, Kumar TR. Targeted disruption of luteinizing hormone beta-subunit leads to hypogonadism, defects in gonadal steroidogenesis, and infertility. Proc Natl Acad Sci U S A 2004; 101:17294–17299.
61. Richards JS, Russell DL, Ochsner S, Espey LL. Ovulation: new dimensions and new regulators of the inflammatory-like response. Annu Rev Physiol 2002; 64:69–92.